Ultrasonics Sonochemistry 22 (2015) 22–29

Contents lists available at ScienceDirect

Ultrasonics Sonochemistry

journal homepage: www.elsevier.com/locate/ultson

Short Communication

Simultaneous sonication assistance for the synthesis of pyrroloacridinones and its efficient catalyst HBF_4 supported on uniform spherical silica nanoparticles

Suman Ray [a], Priyabrata Manna [b], Chhanda Mukhopadhyay [a,*]

[a] Department of Chemistry, University of Calcutta, 92 APC Road, Kolkata 700009, India
[b] Department of Chemical Technology, University of Calcutta, 92 APC Road, Kolkata 700009, India

ARTICLE INFO

Article history:
Received 4 June 2014
Received in revised form 20 June 2014
Accepted 20 June 2014
Available online 30 June 2014

Keywords:
Sonication mediated synthesis
Mesoporous silica nanoparticles
Supported HBF_4 catalyst
Pyrroloacridinones

ABSTRACT

Fluoroboric acid (HBF_4) adsorbed on mesoporous silica nanoparticles of 600 nm dimension was synthesized and characterized by N_2 adsorption, HRTEM, EDX, XPS. The applicability of silica-HBF_4 was probed through the sonication assisted synthesis of pyrroloacridinones in ecofriendly solvent ethanol. Standard leaching experiment was performed to show that the reaction was heterogeneous with this recyclable catalyst.

1. Introduction

Considering the basic green chemistry concepts, ultrasound technique is being proved to be an important tool in the arsenal of "Green Chemistry" [1]. The use of ultrasound for improving the traditional reactions that require longer reaction time, unsatisfactory yields, expensive reagents and high temperature is commonly termed as sonochemistry. "Sonochemistry" is a brand new trend in organic chemistry that shares some aims with green chemistry, with the intention to minimize the environmental impact of chemical synthesis [2]. The phenomenon of piezoelectric effect forms the basis for the production of modern ultrasonic devices [1]. Piezoelectric ceramics generate mechanical vibrations in response to an applied alternating electrical potential and thus generates ultrasonic waves [1]. These ultrasonic waves are propagated *via* alternating compressions and rarefactions cycles, induced in the transmitting liquid through which they pass, with the expansion cycles exerting negative pressure on the liquid [2]. If this applied negative pressure is strong enough to collapse the intermolecular van der Waals force of the liquid, small cavities or gas-filled micro-bubbles are formed which absorb energy from US waves and grow. However, it will reach a stage where it can no longer absorb energy efficiently. Without the energy input, the cavity can no longer sustain itself and implodes [3–5]. These rapid and violent implosions generate short-lived regions with very high local temperature, pressure and heating and cooling rates that can exceed 10 billion °C per second. Such localized hot spots can be thought of as micro reactors in which the mechanical energy of sound is transformed into a useful chemical form that creates an unusual environment for chemical reactions [2–5]. Beside the generation of hot spots, there can also be mechanical effects produced as a result of the violent collapse [2].

In organic synthesis, the two main sources of ultrasound are ultrasonic cleaning baths and ultrasonic immersion probes, which typically operate at frequencies of 40 and 20 kHz, respectively. The formers are more frequently employed in organic chemistry simply because of their low cost and wide availability, even though the amount of energy transferred to the reaction medium is lower than that of ultrasonic probe systems [1,4].

Since proton, H^+ arguably is the most versatile catalyst for organic transformations; the use of Brønsted acid catalysts has high priority from laboratories to chemical manufacturing plants. However following the urgent needs of "green chemistry", an environmentally benign alternative of the homogeneous Brønsted acid catalyst is the supported reagent. In the past several years, some Brønsted acids, such as TfOH, H_2SO_4, HBF_4, $HClO_4$, etc. have been successfully supported onto silica gel and applied as solid acids in various catalytic reactions [6–9]. Ordered mesoporous silica (OMS) is often at the centre of supported heterogeneous catalyst design because of combination of interesting properties such as a high surface area with a robust yet flexible structure and wide

* Corresponding author. Tel.: +91 33 23371104.
E-mail address: cmukhop@yahoo.co.in (C. Mukhopadhyay).

http://dx.doi.org/10.1016/j.ultsonch.2014.06.015
1350-4177/

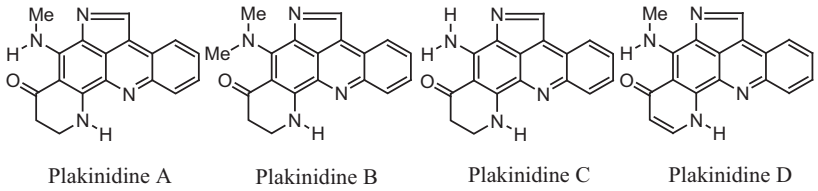

Fig. 1. Biologically active pyrrolo[2,3,4-kl]acridine parent ring containing alkaloids.

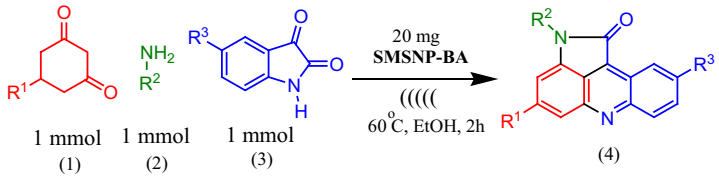

Scheme 1. Ultrasound assisted synthesis of pyrrolo[2,3,4-kl]acridones.

range of compositional variations [10,11]. Moreover, the pore arrangements make them ideal objects for characterization studies, while the pore architecture is usually highly accessible to most common reagents. Such properties are essential for tuning and transforming the composite into a highly performing catalyst. Design and synthesis of surface functionalized ordered mesoporous silica materials have attracted particular attention for their application in catalysis, adsorption, ion-exchange, sensing and so on [12–14]. When such ultrasound assisted synthesis is coupled with the use of heterogeneous catalysis, it fulfills most of criteria of green and sustainable synthesis.

Acridine derivatives were chiefly used as stains for dye manufacturing (e.g., acridine orange) until their fluorescence and chemiluminescence properties found various new applications [15]. Among them, pyrroloacridines and pyrroloacridones are of particular interest because they have a variety of interesting biological activities. Pyrroloacridones are active in assays for anthelmintic, antitumor, antifungal and DNA binding [16–21]. Their abilities to intercalate into DNA are particularly important in inhibiting the growth of cancerous cells, making these compounds ideal for developing novel anticancer drugs [22,23]. Significantly, the pyrrolo[2,3,4-kl]acridine parent ring system is present in some novel pentacyclic alkaloids, Plakinidines A, B, and C (Fig. 1), which were isolated from a Plakortis sponge in 1990 [17,24,25]. Plakinidines A and B exhibited in vitro activity against *Nippostrongylus brastiliensis*, and Plakinidine A showed activity against reverse transcriptase [24]. Only a few reports are available for the synthesis of these molecules, moreover, these methods require multistep syntheses [21,25].

Thus keeping in mind the environmentally benign features of sonochemical assisted synthesis, and in continuation of our interest in sustainable and green synthesis of a wide range of heterocyclic systems [26–31], we herein describe the ultrasound assisted synthesis of uniform spherical mesoporous silica nanoparticle (SMSNP) adsorbed HBF_4 catalysts (**SMSNP-BA**) (600 nm size) and employed them in the synthesis of pyrrolo[2,3,4-*kl*]acridinones (Scheme 1). The nano silica particle has narrow slit-like pores with diameters of 2.4 nm. Albeit, there are plenty of reports on grafting of HBF_4 on mesoporous silica or commercially available silica [8], however, immobilization of HBF_4 on uniform spherical mesoporous silica nanoparticles has not been achieved before.

2. Experimental

2.1. Materials and instrumentation

^{1}H- and ^{13}C-NMR were carried out on Bruker-Advance Digital 300 MHz instrument in $CDCl_3$ or DMSO-d_6 with TMS as internal reference. IR spectra were recorded in KBr pellets in reflection mode on a Perkin-Elmer RX-1 FTIR spectrophotometer. CHN analysis was performed using a Perkin-Elmer 2400 Series II CHN analyzer. Melting points were checked on a Köfler-Block apparatus. Sonication was carried out in TAKASHI ultrasonic cleaning bath (Model No. UD200SH). Nitrogen adsorption/desorption isotherms were obtained using a Quantachrome Autosorb 1C at 77 K. Prior to gas adsorption, all the samples were degassed for 2 h at 353 K. XPS analysis was performed on the Omicron-Nanotech operated at 15 kV and 20 mA using a monochromatic AlK_α as X-ray source. The powder sample was sonicated for 30 min in ethanol and a thin film was prepared by spin coating method which was heated at 120 °C under vacuum before experiment. Transmission electron microscopic images were recorded on a JEOL 2010 TEM operated at 200 kV in Indian Association for the Cultivation of Science, Jadavpur, Kolkata 700 032, India.

2.2. Preparation of uniform spherical mesoporous silica nanoparticles (SMSNP)

In a typical procedure, first, 390 g (390 mL) water and 317 g (400 mL) MeOH was taken in a 1litre open beaker fitted with a magnetic stirrer. Then 3.52 g CTAB was added at room temperature (30–35 °C) and stirred for 30 min. After a clear solution was obtained, tetraethyl orthosilicate (TEOS) was added dropwise from a dropping funnel under stirring condition. Then 10 mL 0.4 N NaOH solution was added drop wise taking 1 h period of time. The stirring was continued for the next 8 h at room temperature and then aged overnight (12–14 h) at room temperature. Then it was filtered and washed thoroughly with deionized water and dried at 35–40 °C for 5 days. The dry powder was calcined at 550 °C for 6–8 h under static air to obtain the uniform spherical mesoporous silica nanoparticles.

2.3. Preparation of silica nanoparticles supported fluoroboric acid (SMSNP-BA)

2.0 g of the as prepared mesoporous silica nanoparticle was dispersed in water (10 mL) in a round bottom flask. 2 mmol of HBF_4 was added to the mixture through a constant-pressure dropping funnel under sonication over a period of 10 min at room temperature. The white solid was collected by filtration. The residue was thoroughly washed with water (5 times) and acetone (5 times). The obtained solid was then dried in vacuum at 50 °C for 2 h and kept in vacuum desiccators. The prepared catalysts were denoted as **SMSNP-BA**.

2.4. General synthesis of the pyrrolo[2,3,4-kl]acridinone derivatives

All the reactions were carried out in round bottomed flask. In a typical reaction a mixture of cyclic-1,3-diketones (**1**) (1 mmol) and different amines (**2**) (1 mmol) in EtOH (4 ml) were placed on an ultrasonic bath and irradiated for 20 min at 60 °C using 20 mg **SMSNP-BA**. Then isatin (**3**) (1 mmol) was added and irradiation was continued for next 100 min at 60 °C. The completion of the reaction was indicated by the disappearance of the starting materials in thin layer chromatography. The products precipitated out once their formation started. After completion of the reaction, the crude product was filtered. The residue contained both the crude product and the catalyst. Then the product was taken in dichloromethane (DCM) and filtered again to separate the product as filtrate from the catalyst (as residue). The DCM was evaporated in rotary evaporator and the crude product was further purified by silica gel column chromatography using EtOAc/petroleum ether (8%/92% v/v) as eluent.

All compounds were synthesized and characterized by IR, NMR, CHN and X-ray single crystal analysis. Spectral data of the unknown compounds are given in the main manuscript and that of all other compounds are given in Supporting Information.

2.4.1. Spectral data of the unknown compounds

*2.4.1.1. 9-bromo-2-p-tolylpyrrolo[2,3,4-kl]acridin-1(2H)-one (**4a**).* Red solid, m.p. 182–184 °C (EtOAc/DCM 1:1); IR (KBr) 2924, 2342, 1710, 1632, 1507, 1458, 1325, 1110, 1078, 825 cm^{-1}; ^1H NMR (300 MHz, $CDCl_3$) δ: 9.05 (1H, d, J = 2.1 Hz), 8.26 (1H, d, J = 9.3 Hz), 7.96 (1H, dd, J = 9 Hz, J = 2.1 Hz), 7.83 (1H, d, J = 9.0 Hz), 7.69 (1H, t, J = 8.7 Hz), 7.49 (2H, d, J = 8.4 Hz), 7.39 (2H, d, J = 8.1 Hz), 6.97 (1H, d, J = 6.9 Hz), 2.47 (3H, s); ^{13}C NMR (75 MHz, $CDCl_3$) δ: 166.7, 150.2, 146.6, 140.3, 137.8, 134.4, 132.1, 131.9, 130.2, 126.6, 126.3, 125.7, 124.4, 123.4, 122.5, 119.9, 106.4, 21.2; Anal. Calcd for $C_{21}H_{13}BrN_2O$: C, 64.80; H, 3.37; N, 7.20. Found: C, 64.84; H, 3.35; N, 7.24.

*2.4.1.2. 2-benzyl-9-bromopyrrolo[2,3,4-kl]acridin-1(2H)-one (**4b**).* Red solid, m.p. 168–170 °C (EtOAc/DCM 1:1); IR (KBr) 3398, 2919, 1710, 1631, 1512, 1461, 1112, 775 cm^{-1}; ^1H NMR (300 MHz, $CDCl_3$) δ: 9.03 (1H, s), 8.24 (1H, d, J = 9.6 Hz), 7.94 (1H, dd, J = 9 Hz, J = 2.1 Hz), 7.75 (1H, d, J = 8.7 Hz), 7.58 (1H, t, J = 7.8 Hz), 7.42–7.28 (5H, m), 6.76 (1H, d, J = 6.9 Hz), 5.16 (1H, s); Anal. Calcd for $C_{21}H_{13}BrN_2O$: C, 64.80; H, 3.37; N, 7.20. Found: C, 64.81; H, 3.36; N, 7.22.

*2.4.1.3. 9-Bromo-2-(3,4-dimethylphenyl)-2H-pyrrolo[2,3,4-kl]acridin-1-one (**4d**).* Red solid, m.p. 192–194 °C (EtOAc/DCM 1:1); IR (KBr) 2922, 2346, 1713, 1631, 1508, 1459, 1323, 1111, 1079 cm^{-1}; ^1H NMR (300 MHz, $CDCl_3$) δ: 9.04 (1H, d, J = 2.1 Hz), 8.27 (1H, d, J = 9.3 Hz), 7.95 (1H, dd, J = 9.0 Hz, J = 2.1 Hz), 7.82 (1H, d, J = 9.0 Hz), 7.68 (1H, t, J = 7.2 Hz), 7.38–7.29 (3H, m), 7.0–6.76 (1H, m), 2.37 (6H, s); ^{13}C NMR (75 MHz, $CDCl_3$) δ: 166.2, 153.0, 149.4, 145.9, 140.0, 137.7, 136.2, 134.1, 133.1, 131.6, 131.5, 130.2, 129.6, 126.6, 125.9, 124.0, 123.0, 122.8 119.5, 114.8, 106.2, 19.6, 19.1; Anal. Calcd for $C_{22}H_{15}BrN_2O$: C, 65.52; H, 3.75; N, 6.95. Found: C, 65.57; H, 3.76; N, 6.91.

*2.4.1.4. 9-Chloro-2-butyl-2H-pyrrolo[2,3,4-kl]acridin-1-one (**4j**).* Red solid, m.p. 132–134 °C (EtOAc/DCM 1:1); IR (KBr) 3060, 2956, 2932, 2874, 2372, 1691, 1631, 1508, 1461, 1307, 1082 cm^{-1}; ^1H NMR (300 MHz, $CDCl_3$) δ: 8.76 (1H, d, J = 2.4 Hz), 8.27 (1H, d, J = 9.0 Hz), 7.79–7.64 (3H, m), 6.86 (1H, d, J = 6.6 Hz), 3.94 (2H, t, J = 7.2 Hz), 1.86–1.76 (2H, m), 1.50–1.42 (2H, m), 0.99 (3H, t, J = 7.2 Hz); ^{13}C NMR (75 MHz, $CDCl_3$) δ: 167.5, 149.9, 146.3, 140.3, 135.5, 133.1, 132.1, 131.8, 127.4, 122.8, 122.0, 120.0, 105.1, 40.4, 30.9, 20.2, 13.7; Anal. Calcd for $C_{18}H_{15}ClN_2O$: C, 69.57; H, 4.86; N, 9.01. Found: C, 69.52; H, 4.88; N, 9.00.

*2.4.1.5. 2-butylpyrrolo[2,3,4-kl]acridin-1(2H)-one (**4k**).* Red solid, m.p. 128–130 °C (EtOAc/DCM 1:1); IR (KBr) 2952, 2931, 2874, 1692, 1631, 1502, 1464, 1301, 1088 cm^{-1}; ^1H NMR (300 MHz, $CDCl_3$) δ: 8.88 (1H, d, J = 8.4 Hz), 8.51 (1H, d, J = 8.4 Hz), 7.94–7.72 (4H, m), 6.91–6.89 (1H, m), 3.95 (2H, t, J = 7.2 Hz), 1.82–1.75 (2H, m), 1.42–1.40 (2H, m), 0.96 (3H, t, J = 7.2 Hz); Anal. Calcd for $C_{18}H_{16}N_2O$: C, 78.24; H, 5.84; N, 10.14. Found: C, 78.21; H, 5.84; N, 10.17.

*2.4.1.6. 9-bromo-2-(3,4-dimethylphenyl)-4-phenylpyrrolo[2,3,4-kl]acridin-1(2H)-one (**4m**).* Red solid, m.p. 234–236 °C (EtOAc/DCM 1:1); IR (KBr) 3428, 1715, 1636, 1498, 1463, 1329, 1128, 1071, 732, 497 cm^{-1}; ^1H NMR (300 MHz, $CDCl_3$) δ: 9.04 (1H, d, J = 1.8 Hz), 8.28 (1H, d, J = 9.6 Hz), 8.00–7.97 (1H, m), 7.69 (2H, d, J = 6.9 Hz), 7.52–7.20 (8H, m), 2.37 (6H, s); ^{13}C NMR (75 MHz, $CDCl_3$) δ: 167.0, 156.6, 147.0, 146.7, 146.6, 140.8, 138.3, 136.7, 134.4, 132.1, 130.7, 129.1, 128.6, 127.6, 127.2, 126.5, 126.4, 124.1, 123.4, 123.3, 119.9, 119.5, 107.3, 20.0, 19.5; Anal. Calcd for $C_{28}H_{19}BrN_2O$: C, 70.15; H, 4.00; N, 5.84. Found: C, 70.18; H, 4.00; N, 5.84.

3. Results and discussion

3.1. Characterization of catalyst

3.1.1. XPS analysis

XPS binding energy profile of the **SMSNP-BA** material is shown in Fig. 2. The peak at 180.6 eV could be assigned due to the presence of B 1s in the material (Fig. 2a). On the other hand the major peak at 691.1 eV could be attributed to the presence of F 1s in **SMSNP-BA** (Fig. 2b) [32]. The broad peaks at 158.5 and 107.6 eV could be attributed to the Si 2s and Si 2p. It confirmed the presence of Si^{4+} with +4 oxidation states with four oxygen neighbors (Figure given in Supporting Information). Further, strong peak at 536.8 eV is responsible for the ejection of electron from O 1s of the covalently bonded oxygen atom. Elemental analysis from the XPS data suggested that the loading of HBF_4 on silica is 0.56 mmol/g. This elemental analysis data further confirms the stoichiometry of F:B at exactly 4.0, and thus mesoporous silica matrix is functionalized with HBF_4 in **SMSNP-BA**.

3.1.2. Nitrogen adsorption analysis

The N_2 adsorption/desorption isotherms and corresponding pore size distribution of silica supported HBF_4 catalyst is shown in Fig. 3. Brunauer–Emmett–Telller (BET) surface area, average pore diameter and pore volume of **SMSNP-BA** are estimated from

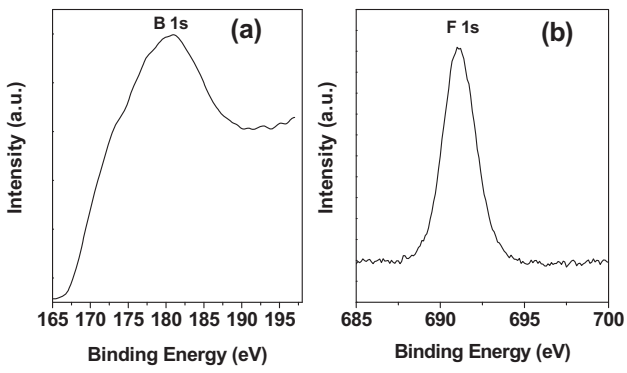

Fig. 2. XPS profile of B1s (a) and F1s (b) of **SMSNP-BA**.

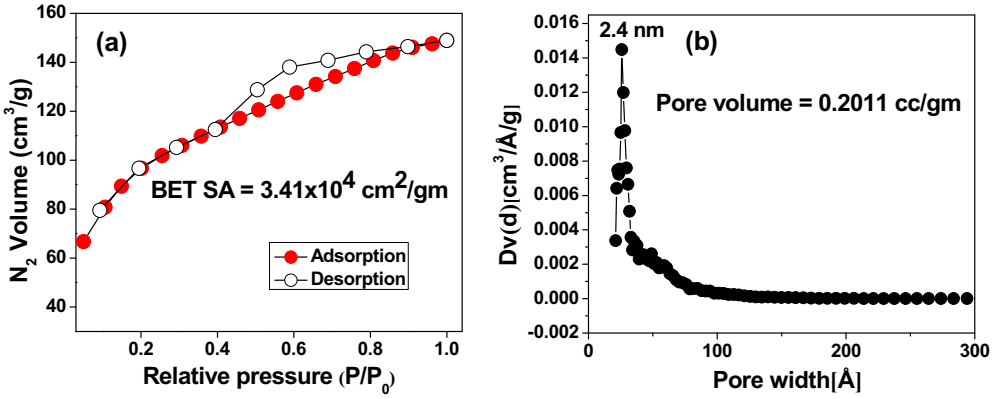

Fig. 3. N_2 adsorption isotherm and pore size distribution of S**MSNP-BA**. Adsorption points are marked by filled circle whereas those for desorption are marked by empty circles.

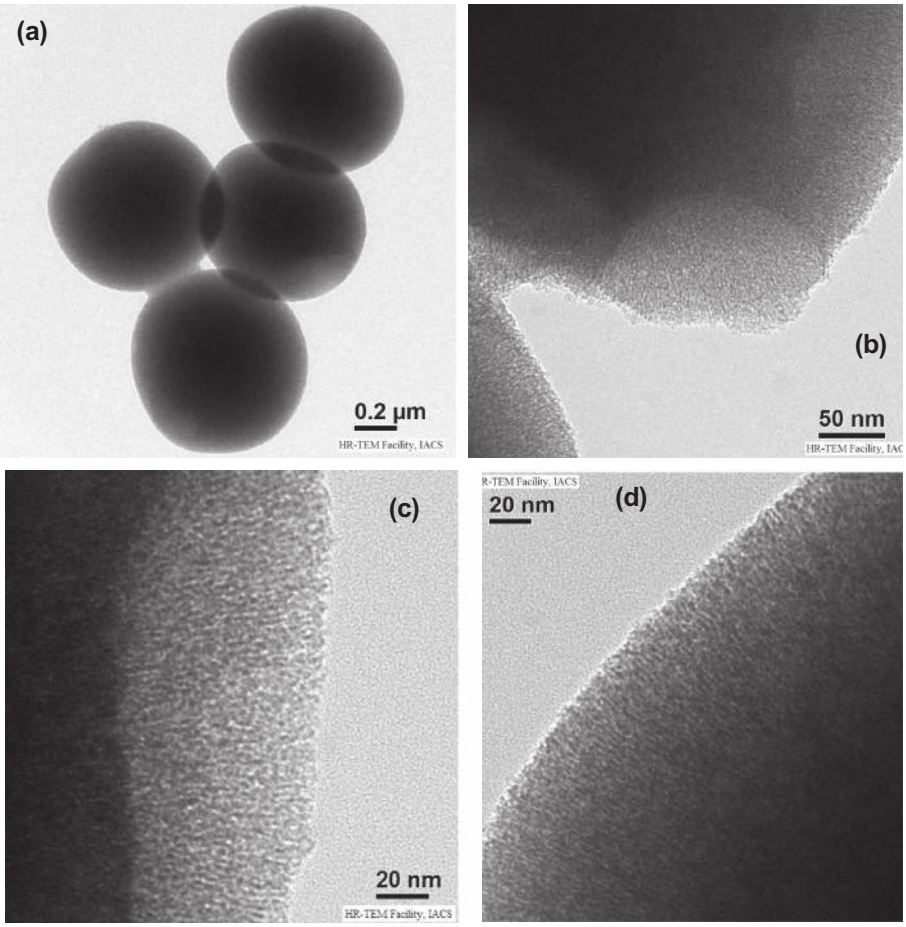

Fig. 4. HRTEM images of **SMSNP-BA** (Panel a, b, c) and SMSNP (Panel d).

the adsorption/desorption isotherms. The isotherm can be classified into typical type IV characteristic (Panel a) of mesoporous materials together with a H4 type hysteresis loop, indicating substantial textural mesoporosity. The BET surface area for **SMSNP-BA** is 3.41×10^4 cm^2/gm and pore volume 0.22 cm^3/gm. Corresponding pore size distribution employing non-local density functional theory (NLDFT) model is shown in the panel b. The pore size distribution shows peaks at 2.4 nm for **SMSNP-BA**. We can find that the surface area of the **SMSNP-BA** (3.41×10^4 cm^2/gm) decreases when compared to pure silica (6.00×10^4 cm^2/g) and pore volume also decreases. Therefore, HBF_4 is adsorbed strongly at the surface of the silica nanoparticles while not fully occupying the total available interparticle space, thereby still leaving room for N_2 adsorption and molecular transport.

3.1.3. HR TEM images of SNSNP-BA

Representative HRTEM images of material **SMSNP-BA** is shown in Fig. 4. As seen from the TEM images the material is composed of uniform spherical particles of dimension *ca.* 600 nm throughout the specimen (Panel a); and on magnification of a particular

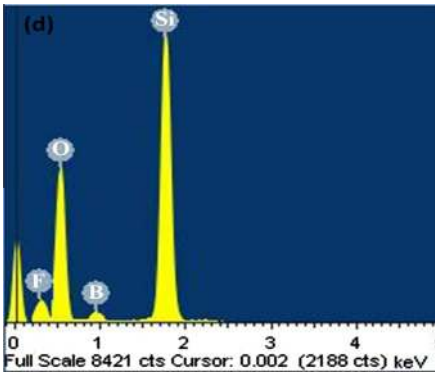

Fig. 5. EDS of S**MSNP-BA.**

spherical nanoparticle the pores (low density spots) of dimension *ca.* 2.4 nm are observable (Panel b, c). Therefore, the mesoporous structure of the host silica material (Panel d) remains intact after modification with HBF_4. These spherical nanoparticles are of tremendous importance for catalytic purpose because spherical shaped nanoparticles have the possibility of larger interparticle void space, which helps easy diffusion of the reactants and products.

In the EDX spectrum (Fig. 5) of **SMSNP-BA**, the small peaks for fluorine and boron clearly indicate that HBF_4 is incorporated within the channels of silica.

3.2. Synthetic application of the catalyst

Multicomponent reactions enable simultaneous cyclization and functionalization making it possible to efficiently prepare diverse derivatives bearing a variety of functionalities. However, this type of multicomponent tandem cyclization requires several reaction components having multiple reaction sites; an unregulated reaction readily forms a complex mixture of undesired products. Therefore, to synthesize the desired compounds selectively, it is extremely important to control the reactions by appropriate choice of the reaction conditions as well as functionality of the substrates. Therefore, to optimize the reaction condition (Table 1), a series of experiments were conducted both under ultrasonic irradiation and conventional heating, taking the reaction of cyclohexane-1,3-dione (1 mmol), 5-bromoisatin (1 mmol) and 3,4-dimethylaniline (1 mmol) as a model reaction. Several common solvents, viz. DCE, DCM, toluene, THF, EtOH, MeOH and water were tested (Table 1). Though the yield of the reaction increased in high boiling and polar-protic solvent than low boiling and aprotic and non polar solvent, the reaction was better in EtOH than in water, possibly due to less homogeneity of the reaction mixture. Therefore ethanol (4 mL) came out as a best choice of solvent. Good to excellent conversion was achieved with different homogeneous acids like HCl, H_2SO_4, $HClO_4$, TfOH, PTS, HPF_6, HBF_4 etc. However, they required repeated work-up, neutralization of strong acids and extensive chromatographic purification. Ultimately the isolated yields were not good (Table 1, entries 1–7). Compared to these homogeneous catalysts, heterogeneous silica supported HBF_4 catalyst afforded better yields of the desired compound (Table 1, entries 8). Similarly, temperature appeared to play a significant role because the yield of pyrroloacridinone was not satisfactory at room temperature (30–35 °C) for conventional heating (Table 1, entries 9). For ultrasound assisted synthesis moderate yield of pyrroloacridinone was obtained at room temperature (Table 1, entries 9). However, the yield was sufficiently high at 55–60 °C under ultrasonic irradiation (Table 1, entries 8). It is pertinent to mention that, in each of the above mentioned reactions the yields of the pyrroloacridinones were always greater for ultrasound assisted synthesis than for conventional heating (Table 1). Thus the best yield, cleanest reaction, and most facile work-up were achieved employing 1.0 equiv of each of cyclohexane-1,3-dione (1 mmol), isatin (1 mmol) and 3,4-dimethylaniline (1 mmol) under ultrasonic irradiation, employing 20 mg of silica supported HBF_4 as the right choice of catalyst and was demonstrated to be the key to obtain good to excellent yields of pyrrolo[2,3,4-kl]acridinones (entry 8). The higher activity of the catalyst under sonochemical conditions can be explained based on higher adsorption and mass transfer of organic molecules on the catalyst surface, which are due to the shockwave and microjets formed [33]. Symmetrical cavitation and symmetrical collapse of bubbles in the liquid medium is very common; however if cavitation bubbles are formed at or near a solid surface the dynamics of cavity collapse change drastically [2]. In homogeneous systems,

Table 1
Optimization reaction conditions.[a]

Entry	Catalyst	Solvent (4 mL)	Temp (°C)	Conventional heating		Ultrasound irradiation	
				%Yield[b]	TOF/h	%Yield[b]	TOF/h
1	HCl	EtOH	55–60	30	14.3	68	42.8
2	H_2SO_4	EtOH	55–60	33	15.6	66	41.7
3	$HClO_4$	EtOH	55–60	35	16.5	70	43.7
4	TfOH	EtOH	55–60	40	18.7	71	43.9
5	PTS	EtOH	55–60	42	19.7	75	44.8
6	HPF_6	EtOH	55–60	45	21.0	76	44.9
7	HBF_4	EtOH	55–60	48	22.4	81	51.1
8[c]	**SMSNP-BA**	EtOH	55–60	60	27.7	95	56.4
9[c]	**SMSNP-BA**	EtOH	30–35	22	10.7	49	28.4
10[c]	**SMSNP-BA**	DCM	25–30	15	7.1	34	22.1
11[c]	**SMSNP-BA**	DCE	55–60	49	22.8	61	40.1
12[c]	**SMSNP-BA**	Toluene	55–60	53	24.6	80	49.9
13[c]	**SMSNP-BA**	Acetone	50–55	15	7.2	38	26.0
14[c]	**SMSNP-BA**	THF	55–60	28	12.3	51	30.7
15[c]	**SMSNP-BA**	MeOH	55–60	43	20.1	62	40.6
16[c]	**SMSNP-BA**	H_2O	55–60	50	23.2	88	53.2

[a] Reaction conditions: Cyclohexane-1,3-dione (1 mmol), 5-bromoisatin (1 mmol), 3,4-dimethylaniline, different catalysts (0.1 mmol for homogeneous catalysts and 20 mg for heterogeneous catalysts), 2 h.
[b] Isolated Yields.
[c] The loading of active site for the silica-HBF_4 catalyst (**SMSNP-BA**) is 0.56 mmol/g.

the cavity remains spherical during collapse because its surroundings are uniform. However, close to a solid boundary, cavity collapse is asymmetric and creates high-speed jets of liquid (with velocities of approximately 10^4 cm/s). These jets hit the surface with tremendous force. This process can produce newly exposed highly reactive catalyst surfaces and increase the mass transfer to the surface of the catalyst [34,35]. Therefore, in the present reaction, the shock waves and high speed jets are probably the reason for the enhancement in the rate and yield of the target molecules under sonic condition.

With the optimized conditions in hand, to delineate this approach, the scope and generality of this protocol was next examined by employing various amines and isatins. An assembly of 14 compounds was synthesized using this protocol (Scheme 2). For precursors **2** bearing either electron-donating or electron-withdrawing substituents on the aromatic ring, the reactions all proceeded very smoothly to provide the corresponding pyrrolo[2,3,4-kl]acridinones. Acid-sensitive methoxy-substituted aryl amines as well as aliphatic amine reacted very efficiently with no side reactions. Therefore, the present silica-fluoroboric acid catalyzed protocol has a general applicability accommodating a variety of substitution patterns. Aromatic amine having substituents in ortho, meta and para positions reacted well to give the corresponding product in excellent yields. The synthetic route is facile, convergent, and allows easy placement of a variety of substituents around the periphery of the heterocyclic ring system. Worth mentioning the product structure was unambiguously proved by X-ray single crystal analysis of **4e** (Fig. 6) (**CCDC 1006462**).

A mechanism portraying the probable sequence of events for the synthesis of pyrrolo[2,3,4-*kl*]acridinones is shown in Scheme 3. It is thought that, the reaction proceeds via a cascade of condensation reactions. Condensation of amine with cyclic-1,3-diketone forms enaminoketone (**5**) which in turn condenses with isatin to give intermediate **7**. Translactamization of **7** affords intermediate **8** which undergoes cyclocondensation to afford intermediate **9**. Subsequent aromatization of intermediate **9** gives the desired product product (**4**).[11a] Compound **5** was also formed by the reaction of cyclic-1,3-diketone with amine in presence of **SMSNP-BA** catalyst in ethanol under ultrasound sonication at 55–60 °C. This compound on reaction with isatin produced the target molecule (**4**). Thus the intermediacy of enaminoketone (**5**) in this reaction is established.

3.3. Catalyst stability and recycling

In order to prove that the reaction is heterogeneous, a standard leaching experiment was conducted. A mixture of dimedone, 5-bromoisatin and 3,4-dimethylaniline in ethanol was allowed to

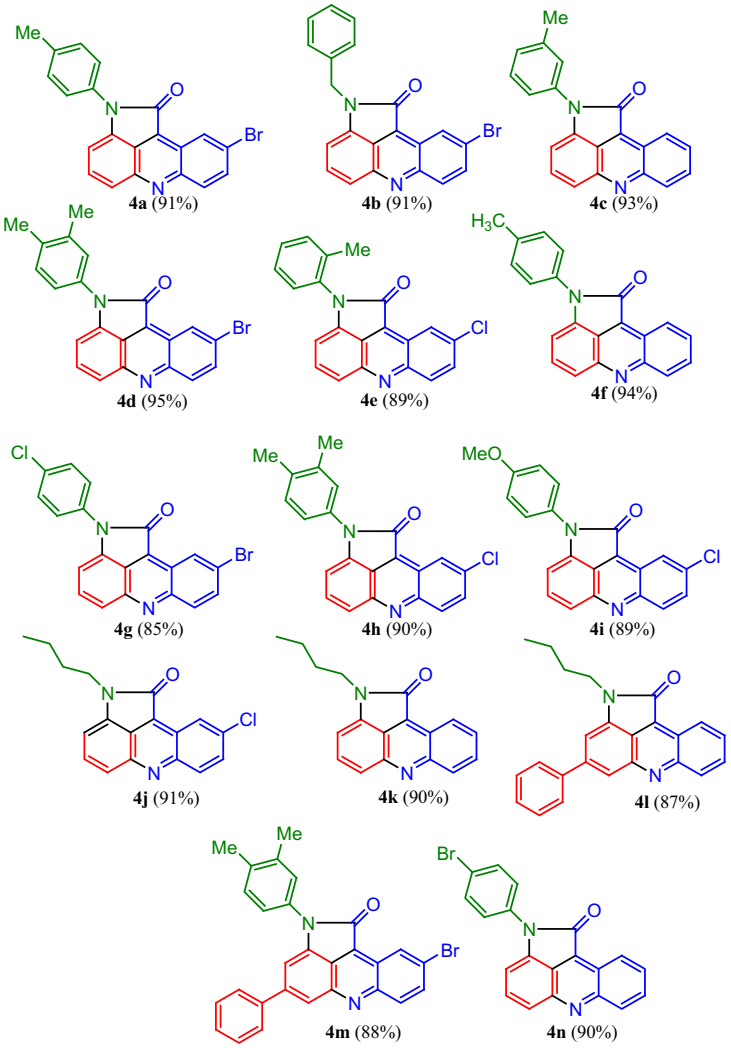

Scheme 2. Structures of the synthesized pyrrolo[2,3,4-kl]acridones.

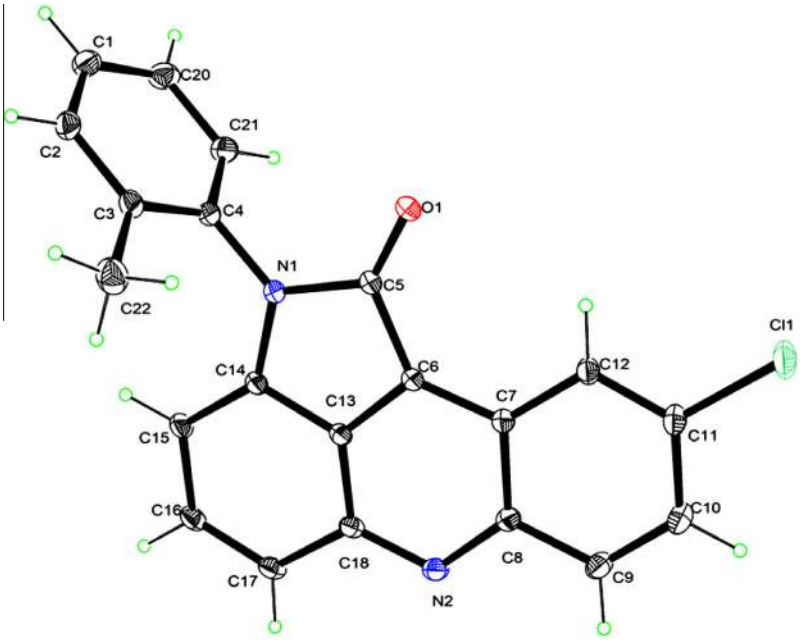

Fig. 6. X-ray single crystal structure of **4e** (**CCDC 1006462**).

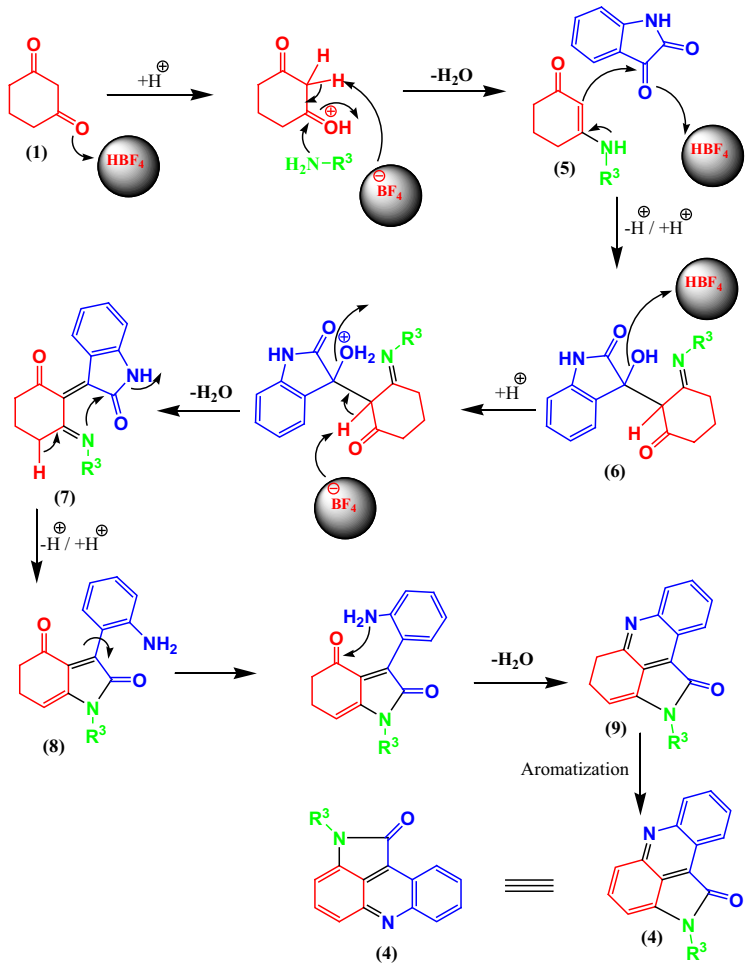

Scheme 3. Probable mechanism for the formation of pyrrolo[2,3,4-kl]acridones.

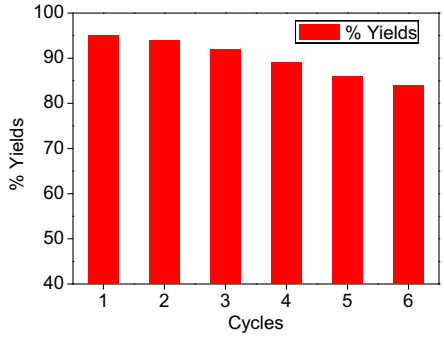

Fig. 7. Yields of pyrrolo[2,3,4-kl]acridinones with reused catalyst.

react for 30 min under ultrasonic irradiation at 60 °C in the presence of **SMSNP-BA** to afford the corresponding pyrrolo[2,3,4-kl]acridinones (**4**). After the 30 min period the reaction mixture was filtered (hot). The filtered reaction mixture was then subjected to ultrasonic irradiation without the catalyst for the next 2 h; no further formation of the corresponding product was observed, indicating that no homogeneous catalyst was involved. XPS analysis of the filtrate showed that HBF_4 was not leached in the solution. The recycled catalyst could be used at least six times. Only a slight decrease in yield was observed (Fig. 7) due to loss of some amount of catalyst during filtration.

4. Conclusion

Therefore, the aim of this protocol is to highlight the synergistic effects of the combined use of organic synthesis under ultrasound mediation in an environmentally benevolent solvent and application of solid acid catalyst for the development of new eco-compatible strategy for fine chemical synthesis.

Acknowledgements

We thank the Council of Scientific and Industrial Research, New Delhi for fellowship (SRF to S.R.). We also acknowledge TEQIP for instrumental facility.

Appendix A. Supplementary data

Supplementary data associated with this article can be found, in the online version, at http://dx.doi.org/10.1016/j.ultsonch.2014.06.015.

References

[1] L. Pizzuti, M. S.F. Franco, A. F.C. Flores, F. H. Quina and Claudio M.P. Pereira, Recent Advances in the Ultrasound-Assisted Synthesis of Azoles, Green Chemistry-Environmentally Benign Approaches (2012), InTech, Available from: <http://www.intechopen.com/books/green-chemistry-environmentally-benign-approaches/recent-advances-inthe-ultrasound-assisted-synthesis-of-azoles>.
[2] R. Cella, H.A. Stefani, Tetrahedron 65 (2009) 2619.
[3] K.S. Suslick, Science 247 (1990) 1439.
[4] T. Mason, J. Chem. Soc. Rev. 26 (1997) 443.
[5] G. Cravotto, P. Cintas, Chem. Soc. Rev. 35 (2006) 180.
[6] P.N. Liu, F. Xia, Q.W. Wang, Y.J. Ren, J.Q. Chen, Green Chem. 12 (2012) 1049.
[7] D. Habibi, M.A. Zolfigol, M. Safaiee, A. Shamsian, A. Ghorbani-Choghamarani, Catal. Commun. 10 (2009) 1257.
[8] D. Kumar, D.N. Kommi, N. Bollineni, A.R. Patel, A.K. Chakraborti, Green Chem. 14 (2012) 2038.
[9] M.I. Ansari, M.K. Hussain, N. Yadav, P.K. Gupta, K. Hajela, Tetrahedron Lett. 53 (2012) 2063.
[10] C.T. Kresge, M.E. Leonowicz, W.J. Roth, J.C. Vartuli, J.S. Beck, Nature 359 (1992) 710.
[11] F. de Clippel, M. Dusselier, S.V. de Vyver, L. Peng, P.A. Jacobs, B.F. Sels, Green Chem. 15 (2013) 1398.
[12] S. Shylesh, Z. Zhou, Q.G. Meng, A. Wagener, A. Seifert, S. Ernst, W.R. Thiel, J. Mol. Catal. A: Chem. 332 (2010) 65.
[13] K. Sarkar, M. Nandi, M. Islam, T. Mubarak, A. Bhaumik, Appl. Catal. A: Gen. 352 (2009) 81.
[14] K. Yamamoto, T. Tatsumi, Chem. Mater. 20 (2008) 972.
[15] N. Desbois, M. Gardette, J. Papon, P. Labarre, A. Maisonial, P. Auzeloux, C. Lartigue, B. Bouchon, E. Debiton, Y. Blache, O. Chavignon, J.C. Teulade, J. Maublant, J.C. Madelmont, N. Moins, J.M. Chezal, Bioorg. Med. Chem. 16 (2008) 7671.
[16] H. Kefayati, F. Narchin, K. Rad-Moghadam, Tetrahedron Lett. 53 (2012) 4573.
[17] W.D. Inman, M. O'Neill-Johnson, P. Crews, J. Am. Chem. Soc. 112 (1990) 1.
[18] E. Gimenez-Arnau, S. Missailidis, M.F.G. Stevens, Anti-Cancer Drug Res. 13 (1998) 431.
[19] P.J. McCarthy, T.P. Pitts, G.P. Gunawardana, M. Kelly-Borges, S.A. Pomponi, J. Nat. Prod. 55 (1992) 1664.
[20] D. Tasdemir, K.M. Marshall, G.C. Mangalindan, G.P. Concepción, L.R. Barrows, M.K. Harper, C.M. Ireland, J. Org. Chem. 66 (2001) 3246.
[21] R. Meesala, R. Nagarajan, Tetrahedron Lett. 51 (2010) 422.
[22] N. Kapuriya, K. Kapuriya, X. Zhang, T.C. Chou, R. Kakadiya, Y.T. Wu, T.H. Tsai, Y.T. Chen, T.C. Lee, A. Shah, Y. Naliapara, T.L. Su, Bioorg. Med. Chem. 16 (2008) 5413.
[23] P. Belmont, I. Dorange, Expert Opin. Ther. Pat. 18 (2008) 1211.
[24] H. Wang, L. Li, W. Lin, P. Xu, Z. Huang, D. Shi, Org. Lett. 14 (2012) 4598.
[25] R.R. West, C.L. Mayne, C.M. Ireland, L.S. Brinen, J. Clardy, Tetrahedron Lett. 31 (1990) 3271.
[26] S. Ray, M. Brown, A. Bhaumik, A. Dutta, C. Mukhopadhyay, Green Chem. 15 (2013) 1910.
[27] S. Ray, A. Bhaumik, M. Pramanik, R.J. Butcher, S.O. Yildirim, C. Mukhopadhyay, Catal. Commun. 43 (2014) 173.
[28] S. Ray, P. Das, A. Bhaumik, A. Dutta, C. Mukhopadhyay, Appl. Catal. A: Gen. 458 (2013) 183.
[29] S. Ray, C. Mukhopadhyay, Tetrahedron Lett. 54 (2013) 5078.
[30] P. Das, A. Dutta, A. Bhaumik, C. Mukhopadhyay, Green Chem. 16 (2014) 1426.
[31] Suman Ray, Paramita Das, Asim Bhaumik, Malay Pramanik, Chhanda Mukhopadhyay, Recycl. Catal. 1 (2014) 34.
[32] J.M. Kinyanjui, D.W. Hatchett, Chem. Mater. 16 (2004) 3390.
[33] A. Javidan, A. Ziarati, J. Safaei-Ghomi, Ultrason. Sonochem. 21 (2014) 1150.
[34] B. Datta, M.A. Pasha, Ultrason. Sonochem. 20 (2013) 303.
[35] J. Safari, Z. Zarnegar, Ultrason. Sonochem. 21 (2014) 1132.